water

Article

Assessment and Improvement of Emergency Rescue Service Accessibility under Urban Waterlogging Disasters

Jiafu Shi, Hao Wang *, Jinjun Zhou and Shuxun Zhang

College of Urban Construction, Beijing University of Technology, Beijing 100124, China; s202164171@emails.bjut.edu.cn (J.S.); zhoujj@bjut.edu.cn (J.Z.); jalezhang@emails.bjut.edu.cn (S.Z.)
* Correspondence: wanghao87@bjut.edu.cn

Abstract: With the acceleration of urbanization and the impact of climate change, the frequent occurrence of urban waterlogging not only leads to road closures and traffic congestion but also severely affects the timeliness of urban emergency rescue. To accurately assess and enhance the response capability of urban emergency rescue under storm-induced waterlogging scenarios, a hydrodynamic model of urban waterlogging was developed to simulate waterlogging conditions under various design rainfall scenarios. By identifying road waterlogging risks and blocked roads, as well as combining the Two-Step Floating Catchment Area (2SFCA) method, the accessibility of emergency rescue services for points of interest (POIs) with different vulnerabilities was evaluated. The Liwan District of Guangzhou City was selected as a case study for accessibility impact assessment and improvement simulation. The results indicate that with the increase in the return period of rainfall, both the area and depth of waterlogged regions increased and the number of roads affected by waterlogging rose, leading to an increase in the length of blocked roads from 11 km to 49 km, an increase of over 300%. Additionally, the number of POIs inaccessible to emergency rescue increased, while the number of accessible POIs decreased, resulting in a significant downward trend in overall accessibility. By deploying mobile pumping vehicles, the depth and area of waterlogging under different rainfall return periods were reduced by over 10%, the number of blocked roads decreased by more than 10%, and the number of accessible POIs increased by more than 12%. The findings highlight that storm-induced waterlogging not only hinders traffic flow but also reduces the response capability of emergency rescue services. Through the strategic deployment of mobile pumping vehicles, the accessibility of urban emergency rescue services under waterlogging conditions can be effectively improved, mitigating the impact of waterlogging on urban functions and public safety.

Keywords: heavy rain and waterlogging; hydrodynamic coupling model; 2SFCA; emergency rescue; accessibility

check for updates

Citation: Shi, J.; Wang, H.; Zhou, J.; Zhang, S. Assessment and Improvement of Emergency Rescue Service Accessibility under Urban Waterlogging Disasters. *Water* **2024**, *16*, 693. https://doi.org/10.3390/w16050693

Academic Editor: Maria Mimikou

Received: 6 February 2024
Revised: 24 February 2024
Accepted: 25 February 2024
Published: 27 February 2024

1. Introduction

In recent years, extreme rainfall events induced by climate change [1], the impact of urban expansion on the natural hydrological cycle [2], changes in the urban surface spatial pattern, and lagging drainage systems [3] have collectively led to frequent urban waterlogging disasters in Chinese cities. Especially in megacities with populations exceeding ten million, the risk of urban flooding is significant [4], and streets and roads face severe challenges. A series of torrential rain and waterlogging events, such as Beijing's "7.21", Wuhan's "7.6", Guangzhou's "5.22", and Zhengzhou's "7.20" [5–8], have profoundly revealed the tremendous impact of waterlogging disasters on urban operations. These events have not only severely damaged urban drainage systems but also caused traffic congestion and the paralysis of city services, posing a significant threat to the livelihood and safety of citizens [9]. It is estimated that about 39% of global traffic infrastructure damage is related to urban flooding [10], with this proportion possibly being higher in China. Urban flooding's impact on the road transportation system is particularly severe, with the damage to roads and streets leading to disruptions in the urban system and affecting daily life. Flood-induced disruptions in the traffic system can result in economic losses exceeding CNY 900 million per hour for each major road [11]. Moreover, the extensive blocking of roads severely affects traffic flow and emergency services, negatively impacting emergency response and rescue operations in flood-affected areas and increasing the difficulty of rescue and treatment. Therefore, under the increasing risk of waterlogging disasters, analyzing the impact of waterlogging on emergency rescue services has become a highly focused issue.

In the assessment of the capability of urban public emergency rescue services, accessibility evaluation is a key indicator [12]. This evaluation comprehensively considers factors such as distance, economic elements, and population models, and uses indicators such as network distance or straight-line distance to measure the ease of accessing resources. In this field, numerous scholars have conducted extensive research and attempts, such as using the gravity model [13], the nearest neighbor distance method [14], average travel time, and the node cost method [15], making significant contributions to the study of accessibility. Particularly, the Two-Step Floating Catchment Area (2SFCA) method, due to its consideration of spatial interactions and supply–demand ratios, has gained attention among scholars in assessing public service capabilities. Some scholars have considered spatial interactions, such as Hu [16] who used the Two-Step Floating Catchment Area (2SFCA) method to analyze the emergency medical services (EMSs) spatial accessibility under different traffic conditions in the central urban area of Shanghai; others considered the supply–demand ratio, such as Zheng [17] and others who chose to use the 2SFCA method to study the spatial utilization of emergency medical services (EMSs) in central Shanghai during multiple heavy rain-induced waterlogging events. Moreover, some scholars have considered both spatial interactions and the supply–demand ratio, like Kiran [18] and others who chose the 2SFCA method to evaluate the traffic accessibility of fire stations and took into account the introduction of a distance–decay function for road network distances, addressing the issue of neglecting the distance–decay factors while considering regional scopes in their research. These studies rely on the 2SFCA method to calculate accessibility, and the computation of the 2SFCA method depends on road network information; in cases of road interruptions caused by heavy rain-induced waterlogging, the accessibility range changes accordingly; thus, accurately identifying blocked roads is crucial for assessing accessibility.

In the process of identifying blocked roads, the simulation of waterlogging is a key step. Numerous researchers have used different waterlogging simulation methods to assess the impact of waterlogging on cities. Some scholars have employed traditional hydraulic models, such as Arrighi [19] and others, who have used the hydraulic model TELEMAC-2D to simulate urban waterlogging, calculating the response times of emergency medical and firefighting services under normal weather and waterlogging scenarios; there are also those who combined hydrological models with geographic information for simulation, like Zhang [20] and others, who utilized the SCS-CN hydrological model in conjunction with GIS spatial analysis to assess the emergency response accessibility of key public services in Jiaozuo city under different flood scenarios. Additionally, a scholar named Luo [21] has conducted a comparative study on various methods of urban flood numerical simulation, elaborating on numerical analysis methods for addressing issues of urban street runoff, architectural obstacles, underground network flow modeling, and feature analysis. It was concluded that the one-dimensional–two-dimensional coupled model, due to its high accuracy in urban flood simulation, has become one of the preferred choices for urban flood modeling. With the rapid development of waterlogging simulation technology, hydrodynamic models have been increasingly applied in waterlogging simulations, effectively improving the accuracy of accessibility assessments impacted by waterlogging disasters.

Enhancing urban accessibility under torrential rain and waterlogging scenarios is key to effectively eliminating waterlogging, thereby reducing road blockages. To achieve this goal, scholars have proposed and studied various methods. Some scholars have used network remodeling to reduce urban waterlogging, including those employing drainage network remodeling, such as Liu [22] who used the Storm Water Management Model (SWMM5.1) with maximum overflow depth, maximum overflow volume, and additional pipeline costs as key indicators to propose a new method for drainage network modification to eliminate urban waterlogging; studies on new drainage systems, such as that by Xiong [23], who proposed a new drainage system optimization method to eliminate urban waterlogging in a case study in Shanghai; and studies using siphon tubes, like Ren [24], who has innovatively proposed a siphonic underground drainage method. Its efficacy was assessed through indoor sandbox experiments and by using the Hydrus-2D model, confirming its effectiveness in eliminating urban waterlogging. These methods all utilize network remodeling and other approaches to reduce urban waterlogging, and there are also scholars who have proposed low-impact development (LID) measures to reduce waterlogging, such as Su [25] and others who, by establishing a two-dimensional coupled model MIKE FLOOD, set up LID combination scenarios and evaluated the water accumulation control effects of each scenario. Wang [26] has used the semi-mountainous area rainwater management model (SWMM) combined with GIS to design various LID scenarios, verifying that LID measures can effectively reduce urban waterlogging to a certain extent. Chen [27] and others have collected urban waterlogging data from Tianjin and proposed a sponge city transformation strategy focused on the old city area to eliminate urban waterlogging. These studies mainly reduce waterlogging through engineering measures, but since road waterlogging is often a local phenomenon, these measures are more suited to improving the overall water management system. Given this, this paper proposes using mobile pump trucks to flexibly reduce waterlogging, enhancing the city's emergency response capability under torrential rain and waterlogging scenarios. This method can more effectively address localized waterlogging, ensuring the smooth flow of urban roads and the accessibility of public services.

This study selected the Liwan District of Guangzhou as the case area and used the SWMM (Storm Water Management Model) and ITF [28] (Integrated Terrestrial Fluxes Model) to construct a one-dimensional and two-dimensional coupled torrential rain and waterlogging model. This study evaluated the accessibility of urban emergency rescue services under torrential rain and waterlogging conditions using the Two-Step Floating Catchment Area (2SFCA) method and simulated the deployment of mobile pump trucks and their drainage effects in practice through the two-dimensional model. The findings of this study provide important references for understanding the impact of waterlogging on the accessibility of urban emergency rescue services and their enhancement strategies.

2. Materials and Methods

2.1. Study Area

This study selected the Liwan District, located in Guangzhou City, Guangdong Province, China, as the research area. The Liwan District is situated in the western central part of Guangzhou, with geographical coordinates ranging from 23°02′ to 23°09′ north latitude and from 113°10′ to 113°15′ east longitude, covering a total area of approximately 59.1 square kilometers. The district is adjacent to the Yuexiu District in the northeast, faces Haizhu District and Panyu District across the river in the southeast, borders the Baiyun District in the north and northwest, and is contiguous with the Nanhai District of Foshan City in the west and south. Due to natural conditions and the urbanization process, Liwan District often faces severe waterlogging issues, especially in low-lying areas and riverside zones, such as Hailong Street, Longjin Street, and Zhongnan Street, where the phenomenon of waterlogging is more pronounced. Figure 1 shows the location map of the study area.

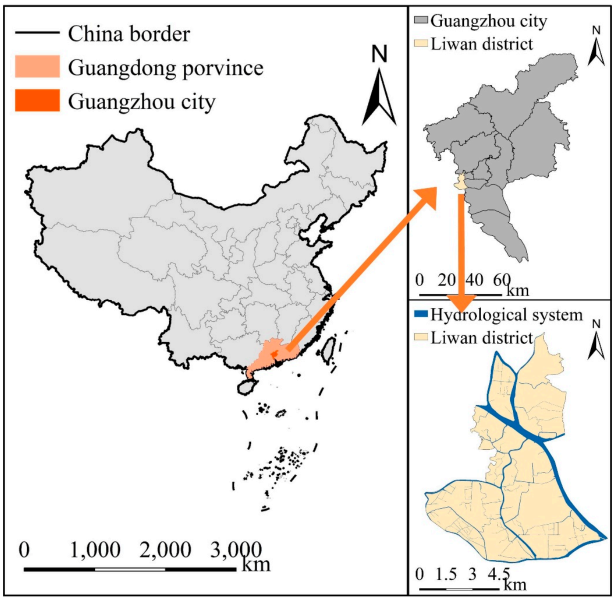

Figure 1. Location map of the study area.

2.2. Urban Waterlogging Model Construction

2.2.1. Model Construction

This study constructed an urban waterlogging drainage hydraulic model using the SWMM (Storm Water Management Model) and ITF (Integrated Terrestrial Fluxes Model). The SWMM 5.1 software includes modules for rainfall evaporation, infiltration excess runoff, overland flow, and network hydraulic calculations, enabling simulation of the urban drainage system's runoff process. The ITF model is used to simulate the two-dimensional overland flow process. By coupling these two models, effective simulation of the waterlogging process can be achieved.

For this paper, basic network data including stormwater pipes, manholes, and drainage outlets were collected and subjected to inspection and correction to remove invalid data and supplement missing segments based on the actual network conditions. The detailed modeling information for the study area's network shows a total length of 998.42 km, comprising 75,658 pipe segments, 77,203 manholes, and 5342 drainage outlets. Figure 2a displays the specific distribution of these networks.

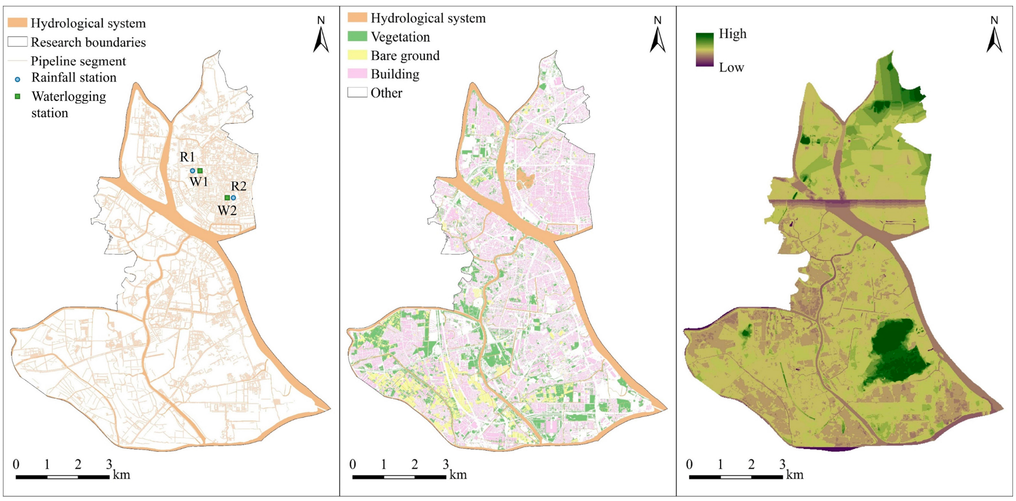

(**a**) Stormwater Network (**b**) Land Use (**c**) DEM Elevation

Figure 2. Distribution maps of stormwater network, land use, and DEM elevation.

This study also included an analysis of land use data such as buildings, vegetation, lakes, bare soil, etc. (as shown in Figure 2b), to extract runoff parameters for sub-catchments, such as roughness coefficients, depression storage, and the proportion of impervious surfaces. The Digital Elevation Model (DEM) raster data, as shown in Figure 2c, has a resolution of 5 m × 5 m and includes building height information. For buildings that have not yet been measured on-site, preset height values were applied to adjust and supplement the elevation data in the DEM, thereby ensuring the model's realism and accuracy. Based on the DEM, we extracted the ground elevations of two-dimensional grid computing units and established a two-dimensional surface flow model with a size of 15 m × 15 m. Finally, the surface two-dimensional flow model was coupled with the network hydraulic model to form a complete one-dimensional–two-dimensional coupled waterlogging model.

2.2.2. Model Accuracy Verification

The urban waterlogging model in this study was primarily validated through surface runoff and drainage parameters. Model accuracy validation used water depth as the core indicator and was based on data from two waterlogging monitoring points within the study area. Rain gauge and waterlogging monitoring stations are both set up in the northern part of Liwan District, specifically on Luhua Street and Duobao Street. The rain gauge stations are labeled as R1 and R2, while the waterlogging monitoring stations are labeled as G1 and G2. The specific locations are shown in Figure 2a. Water depth data were obtained through real-time electronic records monitored by using machines. During periods without rainfall, the water depth monitoring record is updated every 15 min; when water accumulation is first detected, the recording frequency changes to every 1 min; if no water accumulation is detected in the last half hour, the recording interval is adjusted back to every 15 min. A rainfall event with complete data records (24 April 2023) was selected as a case study, comparing the waterlogging process simulated by the model with the actual observed waterlogging process. The assessment of the model accuracy utilized the Nash–Sutcliffe Efficiency Coefficient (NSE) as the evaluation standard. The specific results of the rainfall simulation, the observed waterlogging process, and the Nash–Sutcliffe Efficiency Coefficient are presented in Figure 3.

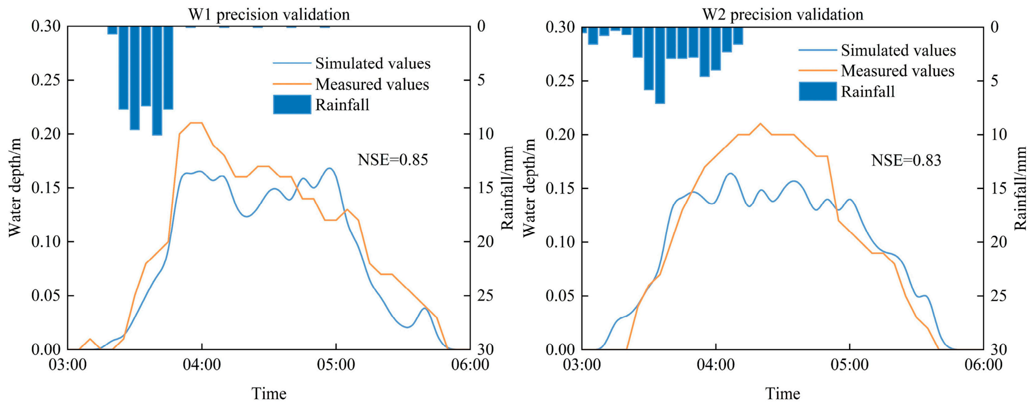

Figure 3. Model verification results for locations W1 and W2 on 24 April 2023.

It is generally considered that a Nash–Sutcliffe Efficiency Coefficient (NSE) greater than 0.8 indicates good model simulation results [29]. Through the analysis of the comparison between simulated and observed waterlogging results, it was found that the model's NSE values are all greater than 0.8, demonstrating that the model has good accuracy.

2.2.3. Design Rainfall

Based on the specific circumstances of Guangzhou, this study utilized the 2 h design rainfall pattern from the "Simplified Technical Report on the Compilation of Storm Intensity Formulas and Design Storm Patterns for Guangzhou City" for the simulation of waterlogging in the study area. The rainfall return periods include 1 year, 5 years, 10 years, 20 years, 50 years, and 100 years, with the corresponding rainfall process charts displayed in Figure 4.

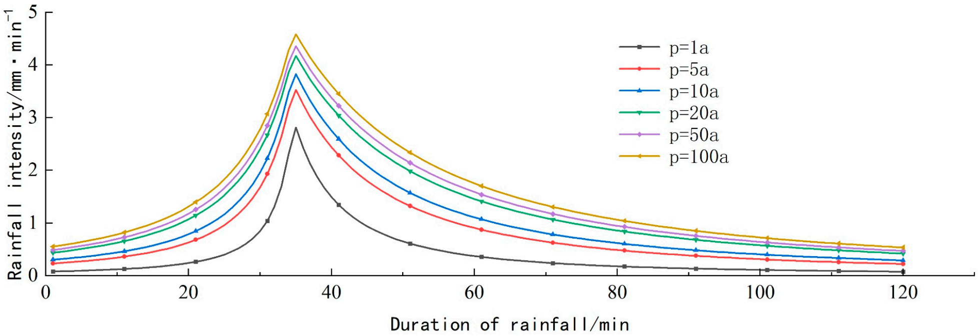

Figure 4. Design rainfall maps for different return periods.

The designed rainfall data were applied to a one-dimensional and two-dimensional hydrodynamic coupled model of storm and waterlogging, simulating scenarios of storm and waterlogging in the Liwan District, Guangzhou City, for return periods of 1 year, 5 years, 10 years, 20 years, 50 years, and 100 years. The simulation duration for each scenario was 2 h.

2.3. Emergency Rescue Accessibility Analysis and Optimization

In storm and waterlogging scenarios, common risks include house collapses, road washouts, and power outages, etc., which seriously threaten people's lives and significantly increase the demand for emergency rescue. Therefore, this study takes firefighting and emergency rescue as an example, considering accessibility in storm and waterlogging scenarios. The specific analysis steps are as follows:

(1) Emergency rescue focus group analysis. Given the timeliness requirements of emergency rescue, this article mainly focuses on the following three types of Points of Interest (POIs) with different vulnerabilities:

High-risk groups: Mainly located in factories, mines, gas stations, and refueling stations. These areas are prone to serious injuries or explosions due to harsh working environments. Based on the timeliness requirement, these POIs are classified as level 3, as key focus objects for emergency rescue.

Vulnerable groups: Including the elderly and children. In torrential rains, these groups are prone to injuries, and are commonly found in nursing homes, nurseries, and kindergartens. Based on the timeliness requirement, these POIs are classified as level 2, as secondary focus objects.

Dense population groups: Cover middle schools, universities, tourist attractions, and commercial centers. Due to the dense flow of people, accidents are prone to occur, increasing the demand for emergency rescue. Therefore, these POIs are classified as level 1, as general focus objects.

See Table 1 for the specific weights and proportions of vulnerable POIs.

Table 1. Vulnerability POI weight table.

POI Type	Number	Proportion	Level
High-risk	86	35.5%	3
Vulnerable	104	42.9%	2
Dense	52	21.6%	1

The distribution of vulnerable population groups is shown in Figure 5a, and the kernel density analysis of the vulnerable population groups is presented in Figure 5b.

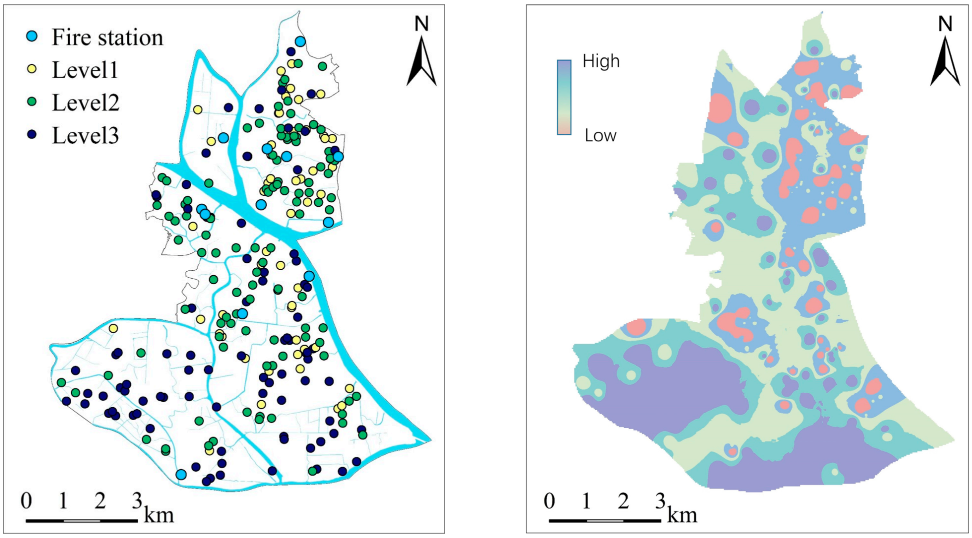

(**a**) Distribution of Vulnerable Population Locations (**b**) POI Kernel Density Analysis

Figure 5. Spatial distribution map of POI weights.

(2) Emergency Rescue Time Threshold Analysis. According to the research by Pons et al. [30], the ideal response time for emergency rescue services is 6 min, while internationally [31], the general time regulation for emergency rescue is set between 8 to 10 min. According to the relevant regulations in Guangzhou City, the maximum time for emergency rescue services to reach the demand location from departure should be 12 min. Taking these standards into account, this article selects 6 min, 9 min, and 12 min as the time thresholds for measuring the accessibility of Points of Interest (POIs) with different vulnerabilities.

(3) Emergency Rescue Supply–Demand Ratio Calculation. Severe storm-induced waterlogging can cause road flooding. Considering that car exhaust pipes are typically located 25 to 35 cm above the ground, road flooding depths greater than 30 cm are designated as impassable, and such roads are marked as obstructed. Due to the lack of real-time road network speed information, traffic congestion and peak traffic conditions are not considered for now. Centering on emergency rescue site j and based on the road network structure and obstructed roads under different designed rainfall conditions, the study searches for the locations of vulnerable POIs that can be reached within the time threshold as the supply domain for each emergency rescue center. Supply scale includes the weighted average of the number of firefighters, fire engines, and firefighting equipment that a fire station can provide. In this article, 1000 was chosen as the supply scale for the fire services [32]. The supply–demand ratio R_j was calculated based on the classification level of POIs to calculate the cumulative demand units within the supply domain as the demand scale. The specific supply–demand ratio R_j calculation formula is as follows:

$$R_j = \frac{S_j}{\left(\sum_{i=1}^{n} D_i\right)} \tag{1}$$

In the formula, S_j represents the supply scale of the emergency rescue station; D_i represents the classification level of demand unit i.

(4) Demand Unit Accessibility Calculation. This was centered on demand unit i, based on the road network structure and obstructed roads under different designed rainfall conditions, searching for fire stations that can be reached within different time thresholds, and summing the supply–demand ratio R_j of the fire stations to obtain the accessibility A_i of each demand point:

$$A_i = \sum_{j=1}^{m} R_j \quad (2)$$

In the formula, A_i represents the accessibility of emergency rescue; R_j represents the supply–demand ratio of emergency rescue.

Based on the above analysis and calculation steps for emergency rescue accessibility, the accessibility in the study area under different designed rainfall return periods and different time thresholds can be obtained, thereby assessing the impact of urban waterlogging disasters on the accessibility of emergency rescue services.

2.4. Optimization of Emergency Rescue Accessibility

Waterlogging often results in road blockages, subsequently affecting the accessibility of emergency rescue services. In such scenarios, conducting an accessibility assessment for the affected areas according to the emergency rescue accessibility calculation process becomes particularly important. When certain areas exhibit low accessibility, improving water management measures can effectively ameliorate this situation. A common method involves using mobile pump trucks (as shown in Figure 6) to promptly eliminate waterlogging, thereby restoring the road's traffic flow. This not only swiftly mitigates the impact of waterlogging but also ensures that rescue vehicles and personnel can timely reach areas requiring assistance, effectively carrying out rescue operations. Mobile pump trucks, with their high lift and large flow characteristics, play an indispensable role in urban drainage work.

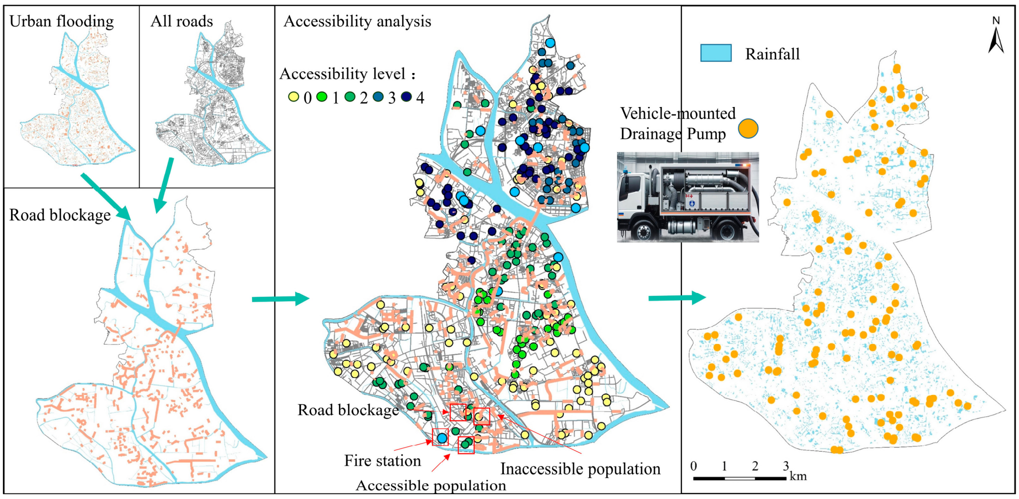

Figure 6. Accessibility impact assessment route map.

The Liwan District in Guangzhou City is equipped with 216 pump trucks, each with a capacity of 300 m^3/h, used to reduce waterlogging and thus enhance urban accessibility. This paper simulates the distribution of mobile pump trucks in Guangzhou in actual scenarios. By utilizing pump trucks to lower water levels on roads, this method reduces road blockages caused by waterlogging, thereby improving the accessibility of affected areas. The placement of pump trucks is based on the waterlogging conditions simulated by the waterlogging model. In the two-dimensional overland flow calculations, integrating the position and function of mobile pump trucks into the model requires clearly identifying the location of the mobile pump trucks within the computational grid of the model. This is achieved by setting a special simulation parameter within the grid cells where the mobile pump trucks are located, which is used to simulate the pumping flow. Figure 6 illustrates the waterlogging accessibility calculation process and the specific arrangement plan for mobile pump trucks. Through this approach, urban waterlogging issues can be more effectively addressed, ensuring smooth traffic and the efficient execution of emergency rescue operations.

3. Results

3.1. Simulation of Spatial Distribution of Waterlogging

This study utilizes an urban waterlogging model to simulate and analyze water accumulation. Based on the urban waterlogging grading standards of Guangzhou City in Guangdong Province, China, this paper classifies waterlogging levels into four categories: minor waterlogging (0–15 cm), light waterlogging (15–30 cm), moderate waterlogging (30–50 cm), and severe waterlogging (over 50 cm).

Through simulation, the maximum waterlogging depth at different time intervals was extracted, allowing for a comparative analysis of the maximum waterlogging depth and distribution of locations before and after waterlogging mitigation (refer to Figure 7). The analysis indicates that areas prone to waterlogging are mainly concentrated in regions with sparse drainage networks. As the rainfall volume increases, waterlogged areas gradually spread to the surrounding regions, enlarging the area of deep water accumulation.

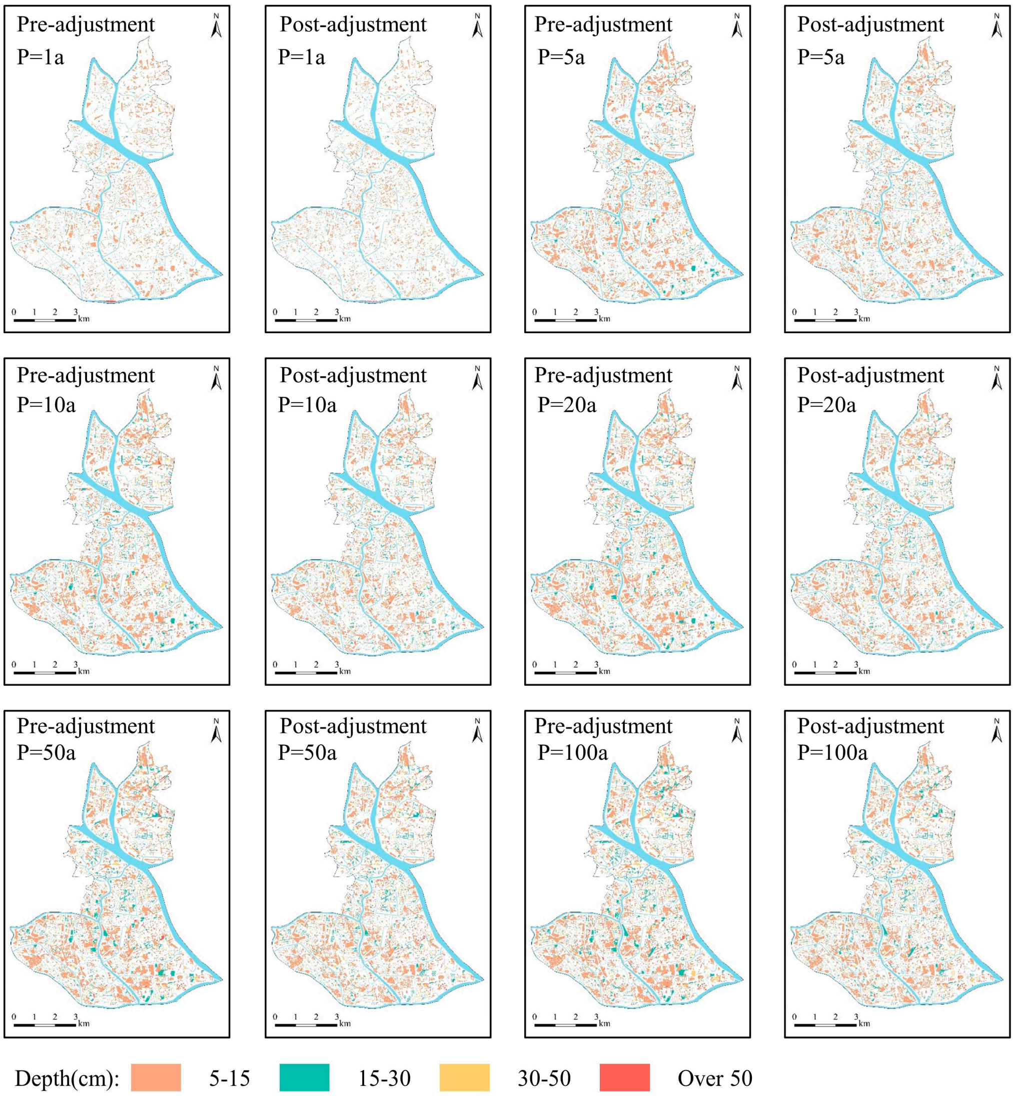

Figure 7. Pre- and post-adjustment water accumulation distribution maps under different return periods.

A comparative chart of waterlogged area before and after improvement under different rainfall return periods was created, as shown in Figure 8. The chart indicates that the waterlogging mitigation measures significantly reduced the area of waterlogging across different rainfall return periods, from a 1-year to a 5-year event. For instance, in the case of a 1-year event, the total area of waterlogging decreased from 6.44 square kilometers to 5.54 square kilometers, a reduction of approximately 13.98%. For higher rainfall return periods, such as a 50-year event, the total area decreased from 15.09 square kilometers to 13.38 square kilometers, a reduction of about 11.33%. Furthermore, in categories of minor, light, and moderate waterlogging, the area of waterlogging also decreased, indicating that the improvement measures are effective in alleviating different levels of waterlogging.

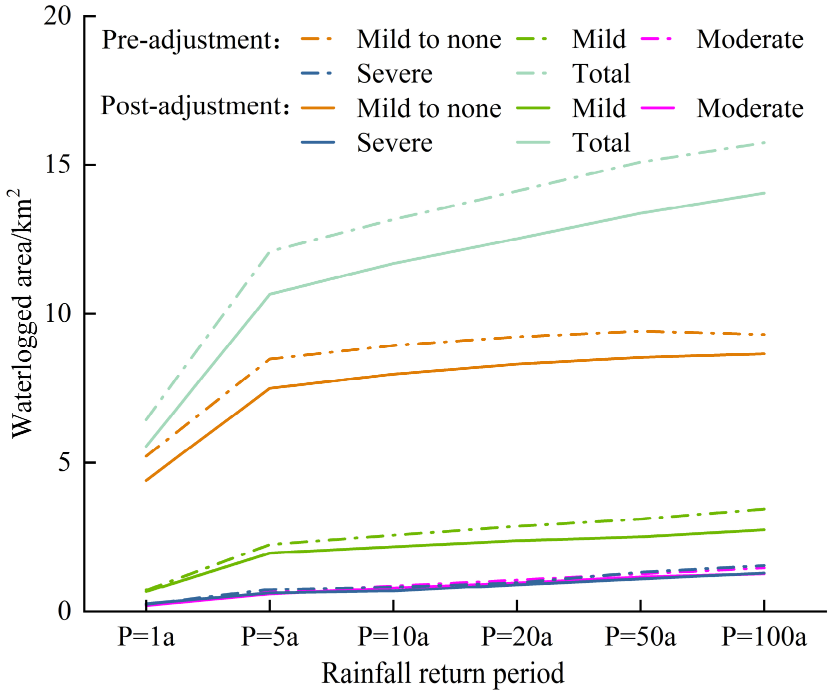

Figure 8. Statistical chart of waterlogged area for different rainfall recurrence periods.

3.2. Analysis of the Impact of Waterlogging on Road Network Blockages

Based on the principles of accessibility calculation, the simulation studying the impact of rainfall on the transportation network compares the changes in blocked roads before and after adjustment under different rainfall return periods, as shown in Figure 9.

Figure 10 shows the changes in the length of blocked roads before and after improvement. The data indicate that the improvement measures can significantly reduce the road closures caused by waterlogging under different rainfall return periods. Specifically, the length of blocked roads for a 1-year return period rainfall decreased from 11.2 km to 6.6 km, and for a 100-year return period, the length decreased from 26.4 km to 22.8 km. As the return period of rainfall extends, the proportion of reduction in improvement effects decreases, from 41.07% in a 1-year event to 13.64% in a 100-year event. This suggests that improvement measures are more effective in mitigating the impact of short-term rainfall, but still provide stable improvement effects in long-term rainfall events.

Figure 9. Pre- and post-adjustment diagrams of obstructed roads.

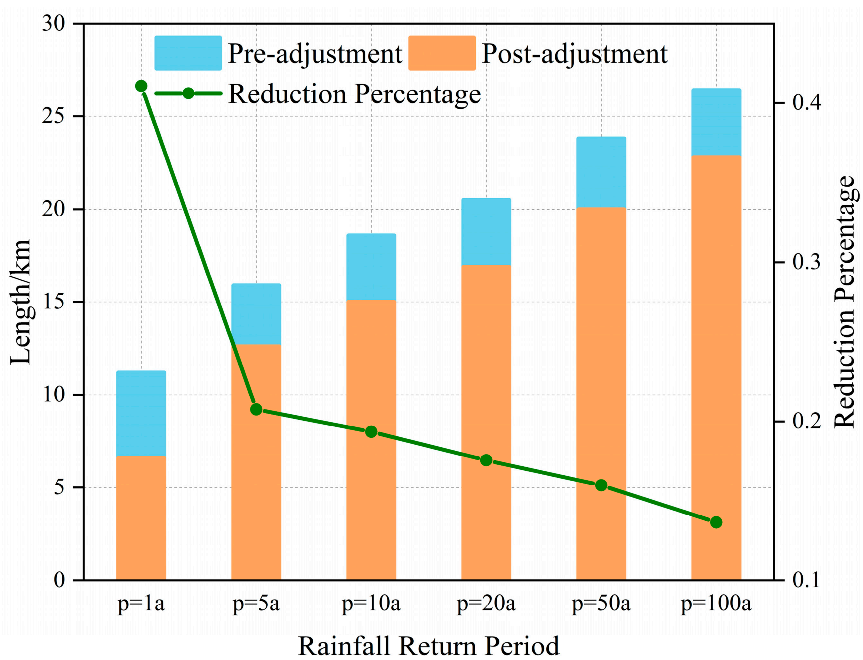

Figure 10. Length of waterlogged roads in different rainfall recurrence periods.

3.3. Emergency Rescue Accessibility Assessment

As described in Section 2.3 of this paper, the accessibility scores calculated using the Two-Step Floating Catchment Area (2SFCA) method were used to measure the number of fire stations accessible to the vulnerable groups in need of fire emergency services. A higher score indicates better accessibility. To illustrate the spatial accessibility changes during different times of the day, this study classified the accessibility scores into five levels, from 0 to 4, with gradually increasing grades. Level 0 refers to areas where emergency rescue cannot reach within the given time threshold. For other areas, level 4 represents the top 25% of accessibility, level 1 represents the lowest 25%, and levels 2 and 3 represent intermediate levels. By applying spatial differential analysis, this paper generated accessibility distribution maps under different weather conditions and time thresholds (as shown in Figures 11 and 12). From the figures, it can be observed that the number of service points (POIs) in areas with low accessibility significantly changed under different time thresholds, while changes in areas with high accessibility were minimal. This may be because areas with high accessibility have fewer blocked roads, so even after improvement, the situation of road blockages changes little compared to the original state, resulting in stable accessibility scores for these areas. Conversely, in areas with low accessibility, some regions are blocked by roads, leading to poor accessibility or even inaccessibility. After improvement, the accessibility of these areas significantly improves.

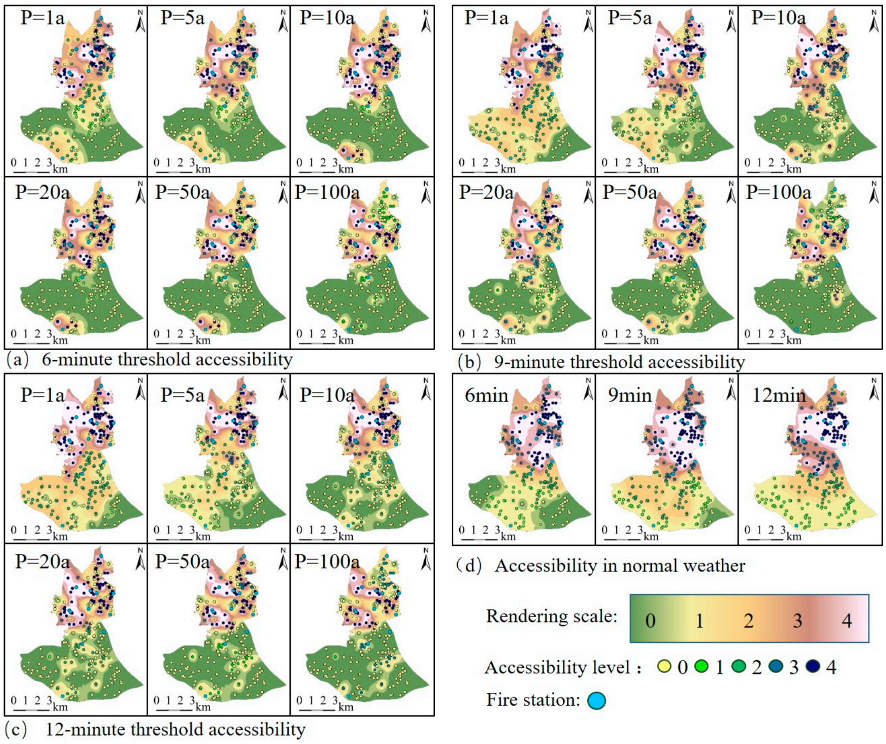

Figure 11. Pre-adjustment accessibility distribution map.

Under normal weather conditions, when the time threshold for emergency rescue services is set to 6 min, the emergency rescue coverage in the study area is only about 80%, with the main uncovered areas located in the southwest and southeast. However, when the time threshold is increased to 9 min and 12 min, most of the previously inaccessible Points of Interest (POIs) become accessible, significantly enhancing the emergency rescue coverage to encompass nearly the entire urban area. This indicates that the accessibility in the southwest and southeast regions is significantly lacking under a 6 min time threshold. Among the POIs inaccessible within this time frame, most are located in high-risk exposure areas, classified as level three in terms of accessibility. Given the high demand for emergency rescue in these areas, strengthening the emergency rescue layout in these regions should be considered.

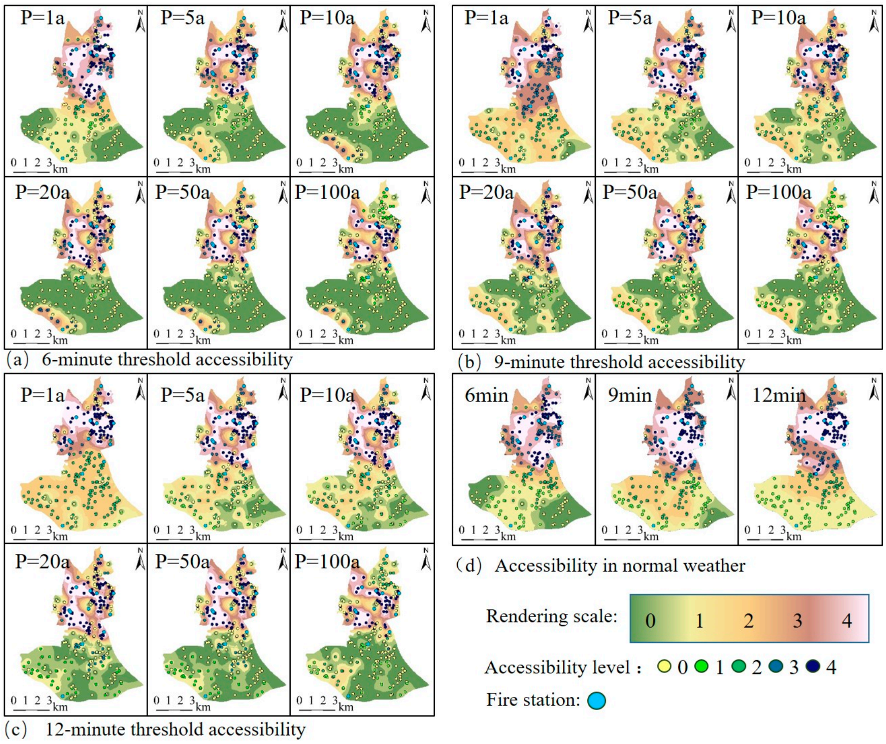

Figure 12. Post-adjustment accessibility distribution map.

Considering different time thresholds and rainfall conditions, due to differences in the spatial distribution of emergency rescue centers, drainage networks, transportation networks, and ground conditions, accessibility distribution shows significant spatial variability. Overall, the northern part of the urban area has higher accessibility, while the southern part has lower accessibility. For instance, locations such as Xinduli Kindergarten, Liwan District Yubi Kindergarten, and Duobao Road Kindergarten in Liwan District, Guangzhou, have higher accessibility due to their proximity to Yongqing Fire Assistance Station and Saiba Road Fire Rescue Station, as well as convenient transportation and comprehensive drainage networks. Conversely, in the southern part, locations such as Baobei Kindergarten, Hainan Kindergarten, and the production department of Guangzhou Damon Construction Technology Co., Ltd. suffer from severely impacted emergency rescue accessibility during extreme rainfall events due to the nearest fire center being more than 3 km away and restricted by poor road network structure.

In this study, the accessibility of fire emergency rescue after the redeployment of mobile pump trucks was assessed (as shown in Figure 13). The analysis focused on the changes in accessibility before and after improvement within 6 min, 9 min, and 12 min intervals. The statistical results show that the average accessibility at a 6 min interval increased from 109 before improvement to 127 after improvement, while the standard deviation increased from 32 to 33, indicating an improvement in average accessibility within short intervals and a similar degree of fluctuation. For a 9 min accessibility, the average increased significantly from 118 to 150, and the standard deviation decreased from 43 to 38, reflecting that the improvement measures enhanced the stability of emergency responses while increasing the average accessibility. Within the 12 min interval, the average accessibility increased from 125 to 157, and the standard deviation decreased from 41 to 37, further proving that the deployment of mobile pump trucks enhanced emergency rescue efficiency and reduced accessibility fluctuations.

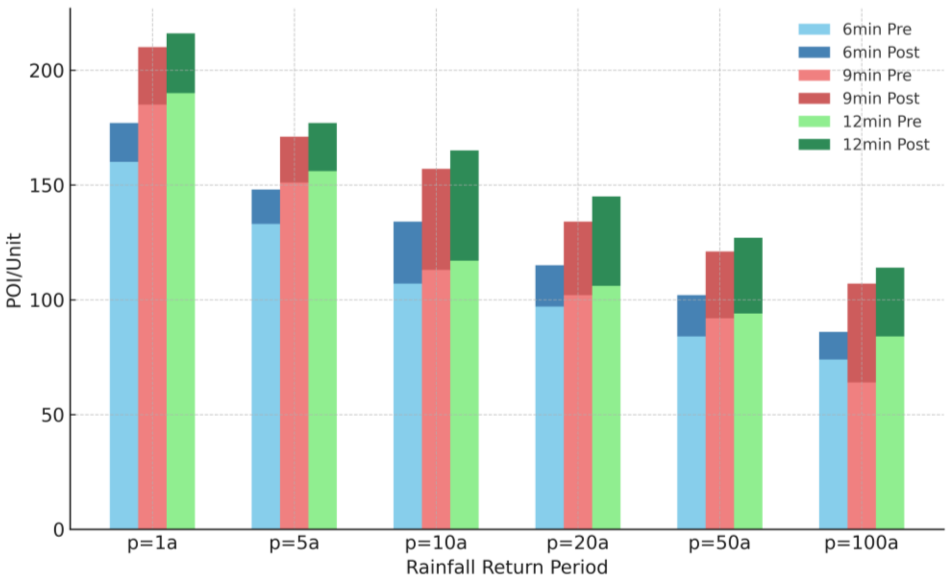

Figure 13. Comparative accessibility chart before and after optimization.

4. Discussion

This study delves into the distribution of waterlogging, road network obstruction, and the accessibility of emergency rescue services through simulation analysis of urban waterlogging under different rainfall return periods in Guangzhou city. The findings hold significant importance for urban flood control planning and the formulation of emergency response strategies.

The results of the waterlogging simulation shown in Figure 8 indicate a clear increase in the area of waterlogging under different rainfall return periods. However, after the deployment of mobile pumping vehicles, the area of waterlogging post-treatment is significantly lower than before. For instance, under the condition of a once-a-year rainfall event, the area of waterlogging decreased from 6.44 square kilometers to 5.54 square kilometers, a reduction of 13.98%. In the case of a 100-year rainfall event, the waterlogged area decreased from 15.09 square kilometers to 13.38 square kilometers, a reduction of 11.33%. The analysis of road blockage situations in Figure 10 shows that the deployment of mobile pumping vehicles significantly reduces road waterlogging and traffic obstruction. From a 1-year to a 100-year return period of rainfall, the length of obstructed roads decreased significantly, from 11.2 km to 6.6 km for a once-a-year event, and from 26.4 km to 22.8 km for a 100-year event. These results not only confirm the significant effectiveness of mobile pumping vehicles in reducing the risk of waterlogging but also highlight the importance of considering both long-term and short-term rainfall events in urban planning. These findings reveal the impact of urban waterlogging on road obstruction and the effectiveness of deploying mobile pumping vehicles to significantly reduce waterlogging and alleviate road obstructions, accurately addressing localized water accumulation.

Further, Figure 13 shows that the analysis of the accessibility of emergency rescue services reveals a general decline in service efficiency and significant disparities in accessibility between regions under extreme weather conditions. Especially in areas with higher vulnerability, extending the rescue time can significantly improve service coverage. For instance, the emergency rescue coverage rate under a 6 min time threshold is only about 80%, mainly excluding areas in the southwest and southeast. However, extending the rescue time threshold to 9 min and 12 min can achieve nearly full coverage of the urban area. This finding is of significant guidance for improving urban disaster response capabilities, suggesting the need for flexibility in time and space in urban planning to enhance emergency response efficiency.

Moreover, the internal spatial differences within the city have a significant impact on the distribution of emergency rescue resources. This study finds that the accessibility in the southern part of the urban area is lower compared to the north, reflecting an imbalance in urban planning and resource allocation. Therefore, enhancing the overall emergency response capability of the city requires not only improving the efficiency of resource allocation but also considering regional disparities to ensure timely and effective rescue in all areas during emergencies.

In this study, the redeployment of mobile pumping vehicles played a crucial role in improving the accessibility of emergency rescue services in the short term. For example, the average accessibility under a 6 min time threshold improved from 109 to 127, indicating that flexible resource allocation strategies are crucial for addressing extreme weather events. This emphasizes the need for dynamic and flexible resource allocation strategies in emergency planning to adapt to changing environments and demands.

In summary, this study not only provides valuable insights into the impact of urban waterlogging on infrastructure and service accessibility but also offers a scientific basis for the development of effective flood control measures and emergency rescue plans. Future research should focus more on optimizing urban infrastructure, especially drainage systems and emergency service resource allocation, to enhance urban resilience to extreme rainfall events. Considering the limitations of model assumptions, such as the inability to fully simulate actual traffic congestion, future studies could further improve the accuracy and applicability of the model based on more realistic factors.

5. Conclusions

This study conducted a detailed simulation and analysis of urban waterlogging in Guangzhou city under different rainfall return periods, yielding several key conclusions. These conclusions not only provide profound insights into the impact of urban waterlogging on infrastructure and accessibility to emergency services but also offer important references for urban planning and disaster response strategy formulation.

(1) Positive correlation between waterlogged area and rainfall return period: This study found that as the rainfall return period increases, the area of urban waterlogging shows an upward trend, both before and after infrastructure enhancement. However, the implementation of infrastructure improvement measures significantly reduces the area of waterlogging, especially in the case of long-term rainfall events, such as those occurring every 20, 50, or 100 years, where the effect of improvement is more pronounced.

(2) Improvement in road blockage situations: The improvement measures significantly reduce road waterlogging and traffic obstruction under different rainfall return periods. There is a significant reduction in the length of obstructed roads from short-term to long-term rainfall return periods, which is crucial for alleviating urban traffic congestion and enhancing city operational efficiency.

(3) Enhancement of emergency rescue service accessibility: Under extreme weather conditions, the efficiency of emergency rescue generally decreases. However, by extending the rescue time threshold, the service coverage rate of emergency rescue can be significantly improved. Moreover, the redeployment of mobile pumping vehicles significantly enhances the average accessibility in a short period, reducing the variability of accessibility.

(4) Consideration of spatial differences in urban planning: This study reveals the impact of internal spatial differences within the city on the distribution of emergency rescue resources, particularly on the lower accessibility in the southern part of the urban area compared to the north. This emphasizes the need to consider such spatial differences in urban planning and emergency resource allocation to ensure timely and effective rescue in all areas during emergencies.

In summary, this study highlights the importance of considering waterlogged areas, road blockage, and accessibility to emergency rescue services in urban flood control planning and emergency management. These findings provide valuable guidance and strategies for city managers in the face of extreme rainfall events. Future research should further explore methods to optimize urban infrastructure and emergency resource allocation to enhance the resilience and response capability of cities to natural disasters. Additionally, studies should also consider the limitations of model assumptions to improve the accuracy and applicability of the research.

Author Contributions: Conceptualization, J.S., J.Z. and S.Z.; Formal analysis, J.S.; Funding acquisition, H.W.; Investigation, H.W.; Methodology, J.S.; Resources, S.Z.; Validation, J.Z.; Writing—original draft, J.S. All authors have read and agreed to the published version of the manuscript.

Funding: This research was funded by the Major Science and Technology Innovation Pilot Project for Water Resources Protection and Integrated-Saving Utilization in the Yellow River Basin of Inner Mongolia Autonomous Region (grant number: 2023JBGS0007), National Natural Science Foundation of China General Project (grant number: 72373011), R&D Program of Beijing Municipal Education Commission (grant number: KM202310005023 &KM202210005017), Beijing Natural Science Foundation (grant number: 8242003).

Data Availability Statement: The data presented in this study are available on request from the corresponding author.

Conflicts of Interest: All authors declare that the research was conducted in the absence of any commercial or financial relationships that could be construed as a potential conflict of interest.

References

1. Taylor, R.G.; Scanlon, B.; Döll, P.; Rodell, M.; Van Beek, R.; Wada, Y.; Longuevergne, L.; Leblanc, M.; Famiglietti, J.S.; Edmunds, M.; et al. Ground water and climate change. *Nat. Clim. Chang.* **2013**, *3*, 322–329. [CrossRef]
2. Hu, D.; Meng, Q.; Schlink, U.; Hertel, D.; Liu, W.; Zhao, M.; Guo, F. How do urban morphological blocks shape spatial patterns of land surface temperature over different seasons? A multifactorial driving analysis of Beijing, China. *Int. J. Appl. Earth Obs. Geoinf.* **2022**, *106*, 102648. [CrossRef]
3. Luo, X.; Liu, P.; Cheng, L.; Liu, W.; Cheng, Q.; Zhou, C. Optimization of in-pipe storage capacity use in urban drainage systems with improved DP considering the time lag of flow routing. *Water Res.* **2022**, *227*, 119350. [CrossRef]
4. Liu, J.; Yang, X.; Ren, S. Research on the Impact of Heavy Rainfall Flooding on Urban Traffic Network Based on Road Topology: A Case Study of Xi'an City, China. *Land* **2023**, *12*, 1355. [CrossRef]
5. Wang, K.; Wang, L.; Wei, Y.-M.; Ye, M. Beijing storm of 21 July 2012: Observations and reflections. *Nat. Hazards* **2013**, *67*, 969–974. [CrossRef]
6. Zhou, C.; Wang, K.; Qi, D. 21. Attribution of the July 2016 extreme precipitation event over China's Wuhan. *Bull. Am. Meteorol. Soc.* **2018**, *99*, S107–S112. [CrossRef]
7. Ruan, J.; Chen, Y.; Yang, Z. Assessment of temporal and spatial progress of urban resilience in Guangzhou under rainstorm scenarios. *Int. J. Disaster Risk Reduct.* **2021**, *66*, 102578. [CrossRef]
8. Huang, X.; Wang, D.; Li, L.Z.; Li, Q.; Zeng, Z. Modeling urban impact on Zhengzhou storm on 20 July 2021. *J. Geophys. Res. Atmos.* **2022**, *127*, e2022JD037387. [CrossRef]
9. Xin, Y.; Jiang, H.; Kong, F.; Lv, L.; Peng, Y. Progress, Problems, and Improving Methods of Non-Engineering Countermeasures Against Urban Meteorological Disasters in China. *Chin. J. Urban Environ. Stud.* **2017**, *5*, 1750004. [CrossRef]
10. Hammond, M.J.; Chen, A.S.; Djordjević, S.; Butler, D.; Mark, O. Urban flood impact assessment: A state-of-the-art review. *Urban Water J.* **2015**, *12*, 14–29. [CrossRef]
11. Lu, X.; Chan, F.K.S.; Chen, W.-Q.; Chan, H.K.; Gu, X. An overview of flood-induced transport disruptions on urban streets and roads in Chinese megacities: Lessons and future agendas. *J. Environ. Manag.* **2022**, *321*, 115991. [CrossRef]
12. Geurs, K.T.; Van Wee, B. Accessibility evaluation of land-use and transport strategies: Review and research directions. *J. Transp. Geogr.* **2004**, *12*, 127–140. [CrossRef]
13. Piovani, D.; Arcaute, E.; Uchoa, G.; Wilson, A.; Batty, M. Measuring accessibility using gravity and radiation models. *R. Soc. Open Sci.* **2018**, *5*, 171668. [CrossRef]
14. Yang, D.-H.; Goerge, R.; Mullner, R. Comparing GIS-based methods of measuring spatial accessibility to health services. *J. Med. Syst.* **2006**, *30*, 23–32. [CrossRef]
15. Yao, B.; Hu, P.; Lu, X.; Gao, J.; Zhang, M. Transit network design based on travel time reliability. *Transp. Res. Part C Emerg. Technol.* **2014**, *43*, 233–248. [CrossRef]
16. Hu, W.; Tan, J.; Li, M.; Wang, J.; Wang, F. Impact of traffic on the spatiotemporal variations of spatial accessibility of emergency medical services in inner-city Shanghai. *Environ. Plan. B Urban Anal. City Sci.* **2020**, *47*, 841–854. [CrossRef]
17. Zheng, M.; Liu, J.; Gao, J.; Zhou, N.; Jiang, S. Measuring Spatial Accessibility to Emergency Medical Services during Rainstorms in Center Shanghai. Available online: https://ssrn.com/abstract=4563102.2023 (accessed on 24 February 2024).
18. Kiran, K.; Corcoran, J.; Chhetri, P. Measuring the spatial accessibility to fire stations using enhanced floating catchment method. *Socio-Econ. Plan. Sci.* **2020**, *69*, 100673.

19. Arrighi, C.; Pregnolato, M.; Dawson, R.; Castelli, F. Preparedness against mobility disruption by floods. *Sci. Total Environ.* **2019**, *654*, 1010–1022. [CrossRef] [PubMed]
20. Zhang, Y.; Li, X.; Kong, N.; Zhou, M.; Zhou, X. Spatial Accessibility Assessment of Emergency Response of Urban Public Services in the Context of Pluvial Flooding Scenarios: The Case of Jiaozuo Urban Area, China. *Sustainability* **2022**, *14*, 16332. [CrossRef]
21. Luo, P.; Luo, M.; Li, F.; Qi, X.; Huo, A.; Wang, Z.; He, B.; Takara, K.; Nover, D.; Wang, Y. Urban flood numerical simulation: Research, methods and future perspectives. *Environ. Model. Softw.* **2022**, *156*, 105478. [CrossRef]
22. Liu, Y.; Zhao, W.; Wei, Y.; Sebastian, F.S.M.; Wang, M. Urban waterlogging control: A novel method to urban drainage pipes reconstruction, systematic and automated. *J. Clean. Prod.* **2023**, *418*, 137950. [CrossRef]
23. Xiong, L.; Lu, S.; Tan, J. Optimized strategies of green and grey infrastructures for integrated control objectives of runoff, waterlogging and WWDP in old storm drainages. *Sci. Total. Environ.* **2023**, *901*, 165847. [CrossRef]
24. Ren, X.; Wang, S.; Yang, P.; Tao, Y. Experimental and modeling evaluation of siphon-type subsurface drainage performance in flooding and waterlogging removal. *Agric. Water Manag.* **2023**, *275*, 108031. [CrossRef]
25. Su, J.; Li, J.; Gao, X.; Yao, Y.; Jiang, C. Comprehensive analysis of waterlogging control and carbon emission reduction for optimal LID layout: A case study in campus. *Environ. Sci. Pollut. Res.* **2022**, *29*, 87802–87816. [CrossRef]
26. Wang, D.; Fu, X.; Luan, Q.; Liu, J.; Wang, H.; Zhang, S. Effectiveness assessment of urban waterlogging mitigation for low impact development in semi-mountainous regions under different storm conditions. *Hydrol. Res.* **2021**, *52*, 284–304. [CrossRef]
27. Chen, W.; Dong, J.; Yan, C.; Dong, H.; Liu, P. What Causes Waterlogging?—Explore the Urban Waterlogging Control Scheme through System Dynamics Simulation. *Sustainability* **2021**, *13*, 8546. [CrossRef]
28. Huang, H.; Liao, W.; Lei, X.; Wang, C.; Cai, Z.; Wang, H. An urban DEM reconstruction method based on multisource data fusion for urban pluvial flooding simulation. *J. Hydrol.* **2023**, *617*, 128825. [CrossRef]
29. Lin, F.; Chen, X.; Yao, H. Evaluating the use of Nash-Sutcliffe efficiency coefficient in goodness-of-fit measures for daily runoff simulation with SWAT. *J. Hydrol. Eng.* **2017**, *22*, 05017023. [CrossRef]
30. Pons, P.T.; Haukoos, J.S.; Bludworth, W.; Cribley, T.; Pons, K.A.; Markovchick, V. Paramedic response time: Does it affect patient survival? *Acad. Emerg. Med.* **2005**, *12*, 594–600. [CrossRef] [PubMed]
31. Shi, Y.; Yao, Q.; Wen, J.; Xi, J.; Li, H.; Wang, Q. A spatial accessibility assessment of urban tourist attractions emergency response in Shanghai. *Int. J. Disaster Risk Reduct.* **2022**, *74*, 102919. [CrossRef]
32. Yin, J.; Yu, D.; Liao, B. A city-scale assessment of emergency response accessibility to vulnerable populations and facilities under normal and pluvial flood conditions for Shanghai, China. *Environ. Plan. B Urban Anal. City Sci.* **2021**, *48*, 2239–2253. [CrossRef]